Akinori Tamura[1]
Hitachi Europe Limited,
7th Floor, Capital House,
25 Chapel Street,
London NW1 5DH, UK
e-mail: akinori.tamura.mt@hitachi.com

Chenghuan Zhong
Inductosense Ltd.,
Engine Shed,
Station Approach,
Bristol BS1 6QH, UK
e-mail: bamboo@inductosense.com

Anthony J. Croxford
Department of Mechanical Engineering,
University of Bristol,
Queen's Building,
University Walk,
Bristol BS8 1TR, UK
e-mail: a.j.croxford@bristol.ac.uk

Paul D. Wilcox
Department of Mechanical Engineering,
University of Bristol,
Queen's Building,
University Walk,
Bristol BS8 1TR, UK
e-mail: p.wilcox@bristol.ac.uk

A Feasibility Study of Noncontact Ultrasonic Sensor for Nuclear Power Plant Inspection

A pipe-wall thinning measurement is a key inspection to ensure the integrity of the piping system in nuclear power plants. To monitor the integrity of the piping system, a number of ultrasonic thickness measurements are manually performed during the outage of the nuclear power plant. Since most of the pipes are covered with an insulator, removing the insulator is necessary for the ultrasonic thickness measurement. Noncontact ultrasonic sensors enable ultrasonic thickness inspection without removing the insulator. This leads to reduction of the inspection time and reduced radiation exposure of the inspector. The inductively-coupled transducer system (ICTS) is a noncontact ultrasonic sensor system which uses electromagnetic induction between coils to drive an installed transducer. In this study, we investigated the applicability of an innovative ICTS developed at the University of Bristol to nuclear power plant inspection, particularly pipe-wall thinning inspection. The following experiments were performed using ICTS: thickness measurement performance, the effect of the coil separation, the effect of the insulator, the effect of different inspection materials, the radiation tolerance, and the measurement accuracy of wastage defects. These initial experimental results showed that the ICTS has the possibility to enable wall-thinning inspection in nuclear power plants without removing the insulator. Future work will address the issue of measuring wall-thinning in more complex pipework geometries and at elevated temperatures. [DOI: 10.1115/1.4035466]

Introduction

Many piping systems, such as within an oil and gas system, a chemical plant, a fossil-fuel power plant, a nuclear power plant, etc., are subject to corrosion and erosion which cause thinning of the pipe-wall. In order to ensure the integrity of the piping system, it is important to evaluate the wall thickness and the wall-thinning rate, and ultrasonic measurements are often used for this. Recently, a high temperature monitoring system [1] and data processing technique [2] have been developed for the inspection of oil and gas systems.

Nuclear power plants can also experience problems due to pipe-wall thinning such as the Surry Unit 2 in 1986 [3] and Mihama Unit 3 in 2004 [4]. Following these incidents, a number of research programs were conducted to evaluate the wall-thinning problem [5–10]. Ultrasonic thickness measurements are now commonly used for inspection of pipe-wall thinning of nuclear power plants.

In Japan, numerous ultrasonic thickness measurements are manually carried out during the outage of a nuclear power plant. Since most of the pipes are covered with an insulator, removing the insulator is necessary before inspection of the pipe-wall. After removing the insulator, a skilled inspector carries out the ultrasonic thickness measurement by attaching the ultrasonic probe to each measurement point on the pipe surface. After that, the insulator has to be re-installed on the pipe again.

Recently, noncontact ultrasonic measurement techniques have been proposed by a few research groups [11–18]. In these noncontact ultrasonic measurements, the data from the transducer, which is attached to the inspection target, is transferred by wireless communication (e.g., Wi-Fi and so on) or electromagnetic induction. The noncontact ultrasonic sensor based on electromagnetic induction between coils was first introduced by Greve et al. [15]. The proposed noncontact method, known as an inductively-coupled transducer system (ICTS), has an advantage against other noncontact methods in that electricity is not required in the sensor attached to the inspection target. The data is transferred by electromagnetic induction, and therefore, connecting cables (required for other methods) are not required.

Zhong et al. from the University of Bristol [17] proposed an innovative ICTS based on a three-coil electrical circuit model, in which the input and output voltage can be individually controlled by changing the coil parameters. By optimization of the three coil parameters, the maximum coil separation, which corresponds to the maximum noncontact measurement distance, has been significantly improved and they have demonstrated a 40 mm separation between the coils in composite materials [18].

If the ICTS is to be applicable to pipe-wall thinning inspection of a nuclear power plant, the inspector needs to be able to carry out the ultrasonic thickness measurement through the insulator without removing it. Leaving the insulator on the pipe leads to a reduction of the inspection time and the exposure of radiation to the inspector (as radiation exposure depends on the inspection time and the distance between the inspector and the radiation source). Similarly, the permanently-installed sensor can increase the reliability of measurements. However, it remains to be shown if such a system is suitable for nuclear plant inspection.

In this study, we investigate the applicability of the University of Bristol ICTS to inspection of wall-thinning of the nuclear power plant. The following experiments were performed: thickness measurement performance, the effect of coil separation, the effect of the insulator, the effect of different inspection material, radiation tolerance, and measurement accuracy for wastage defects. Thickness measurements using ICTS have not previously been reported [17,18] and as a first step, we confirm the thickness measurement performance of the ICTS. In the experiments

[1]Corresponding author.

Manuscript received June 23, 2016; final manuscript received November 30, 2016; published online March 1, 2017. Assoc. Editor: John F. P. de Grosbois.

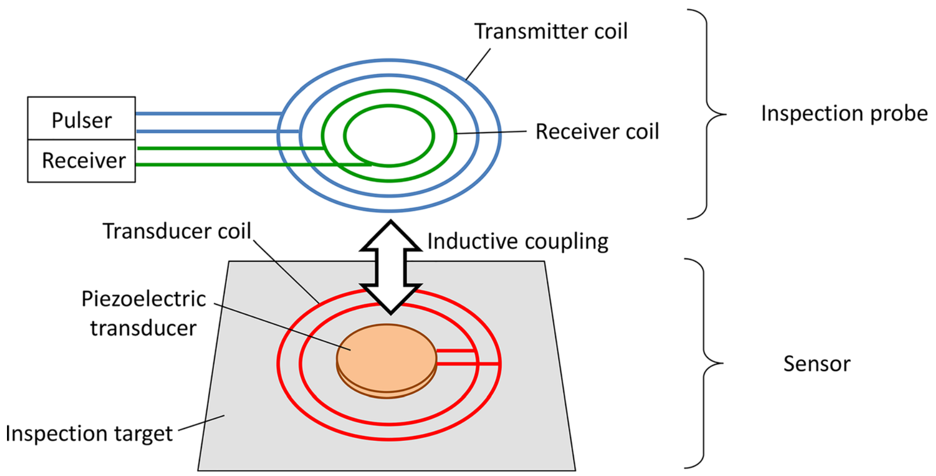

Fig. 1 Concept of the inductively coupled transducer system

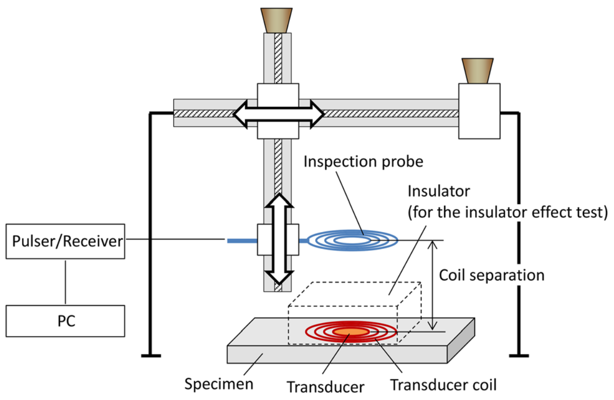

Fig. 2 A schematic view of the experimental apparatus

regarding the coil separation and the insulator, we investigate the possibility of pipe inspection without removing the insulator. The transducer side of the ICTS, which is explained in the Experimental Methodology and Apparatus section, is installed on the pipe surface for a long time period. Hence, it is essential to confirm the radiation tolerance of ICTS for nuclear power plant inspection. We look into this in the radiation tolerance tests. It is known that liquid droplet impingement erosion (LDI) causes local wall thinning. This means that the shape of the LDI defect becomes narrow and deep compared to that of flow accelerated corrosion (FAC). In the experiments regarding the measurement accuracy for the wastage defects, we confirm the applicability to the inspection of the LDI defects.

For inspections of the high temperature piping system of the nuclear power plant, the high temperature durability of the sensor is indispensable. The high temperature durability strongly depends on the bonding method. Thus, in this study, we do not investigate the high temperature durability in order to focus on the investigation of the inherent characteristics of the ICTS.

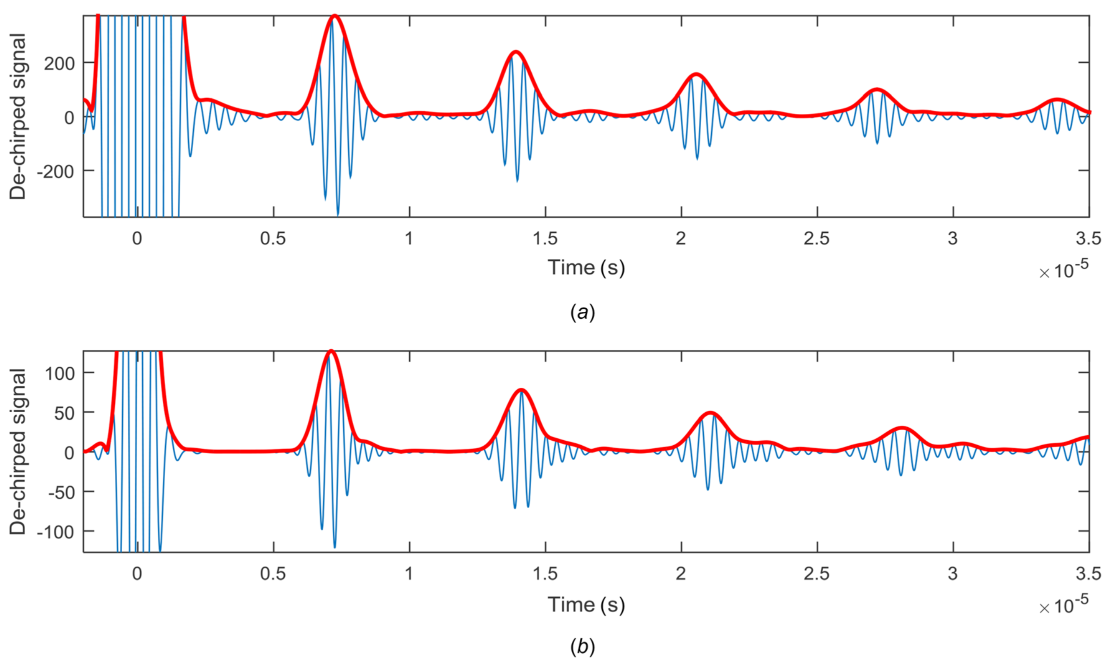

Fig. 3 The comparison of the dechirped signals in 20 mm thickness measurement: (*a*) conventional ultrasonic sensor and (*b*) ICTS (coil separation: 35 mm)

Experimental Methodology and Apparatus

In this section, we describe the ICTS which is tested in this research. We also explain the experimental methodology and the experimental apparatus.

Noncontact Ultrasonic Sensor. Figure 1 illustrates the ICTS concept proposed by Zhong et al. at the University of Bristol [17,18]. It consists of two parts, a sensor and inspection probe. The sensor is embedded or bonded to the surface of the inspection target. The sensor has a transducer coil and a piezoelectric transducer, which are connected to each other. It should be noted that the sensor is passive, that is, it does not require any electricity by cables or contain batteries. The inspection probe contains a transmitter coil and a receiver coil. The transmitter coil and the receiver coil are, respectively, connected to a pulser and a receiver. A conventional pulser and receiver can then be used to drive the ICTS or bespoke solutions. The sensor and the inspection probe are physically separated as shown in Fig. 1, but they are inductively coupled with each other.

In the inspection by the ICTS, the input signal controlled by the pulser is inductively transmitted to the transducer coil via the transmitter coil. And then, the input signal is converted into bulk ultrasonic waves by the piezoelectric transducer. The generated bulk ultrasonic waves, which are the longitudinal waves in this study, are reflected from the bottom wall or the defects in the inspection target. The reflected ultrasonic waves are converted into the electrical signal (the output signal) by the piezoelectric transducer. The output signal is inductively transmitted to the receiver coil from the transducer coil. Finally, the output signal is recorded by a data logger, which is connected to the receiver.

The piezoelectric transducer (NCE51—Noliac Denmark) was formed in a disk-shape and a frequency of 2 MHz was used. The coil parameters, the outer diameter, the inner diameter and the number of turns, are optimized for operation at 2 MHz by the three-coil coupling circuit model (outlined in Refs. [17] and [18]). The outer diameter of the coils is the most effective parameter for improving the performance of the ICTS and in this study outer coil diameters of 50 mm was used, essentially defining the size of the sensors.

Experimental Apparatus. In order to carry out the experiments regarding the above mentioned test items, the experimental apparatus shown in Fig. 2 is used in this study. The inspection probe is fixed on the rail of the experimental equipment to freely control its position and the pulser and the receiver, Handyscope (HS3, TiePie Engineering, Sneek, Netherlands) is connected to it. The transducer coil and the piezoelectric transducer are bonded to the surface of the specimen. For the tests using insulators, the insulator is placed between the transducer side and the inspection probe, but the insulator is removed in the other tests.

To increase the signal to noise ratio (SNR), a chirp signal is used as the input signal [19]. The chirp signal S is described by the following equation:

$$S(t) = w(t) \cdot \sin\left(2\pi\left(f_c - \frac{B}{2}\right)t + \frac{\pi B t^2}{T}\right) \quad (1)$$

where f_c is the central frequency, T is the duration of the chirp, and B is the chirp bandwidth. The window function $w(t)$, having a unit amplitude, starts at $t=0$ and ends at $t=T$. The desired response, which is the response to a tone burst wave in this study, is obtained from the frequency domain deconvolution of the received signal. For the detail of this data processing, see Ref. [19]. Hereafter, the data-processed signal is referred as dechirped signal. In this study, the central frequency is set at 2 MHz, which is mainly used for nuclear power plant inspection.

Experiment Results and Discussion

In this section, we discuss the experiment results and the applicability of the ICTS to nuclear power plant inspection.

Thickness Measurement Performance. Thickness measurements using ICTS have not previously been reported [17,18], and we first confirm the performance of the ICTS for thickness inspection using longitudinal ultrasonic waves. In these experiments, the coil separation is fixed at 35 mm where the SNR becomes sufficiently high (more than 400). There is no insulator between the inspection probe and the transducer. In nuclear power plants, the pipe material is mainly carbon steel. Hence, carbon steel plates are used as the specimens in this study. The thicknesses of the specimens in these experiments are 3.6, 7.7, 9.5, 19.7, and 49.5 mm. This covers most inspection target thickness in wall-thinning inspection of the nuclear power plant.

The dechirped signals obtained from the ICTS and a conventional ultrasonic sensor is compared in Fig. 3. The blue lines represent the dechirped signals and the red lines show the signal envelopes which are calculated by the Hilbert transform of the dechirped signals. There is good agreement between the conventional ultrasonic sensor and the ICTS. In order to investigate the

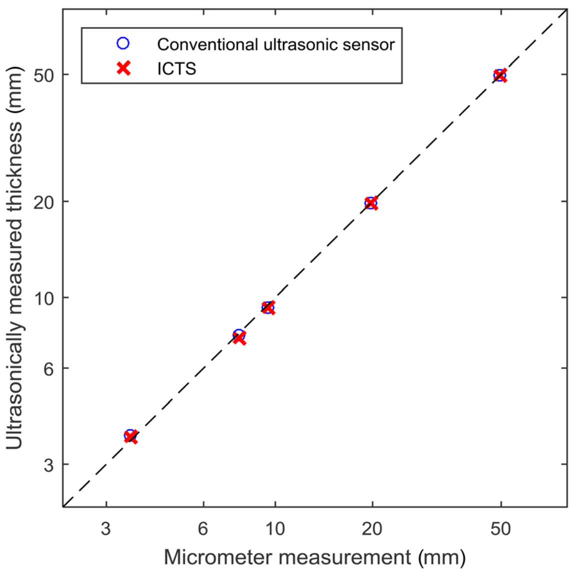

Fig. 4 The thickness measurement performance of the ICTS

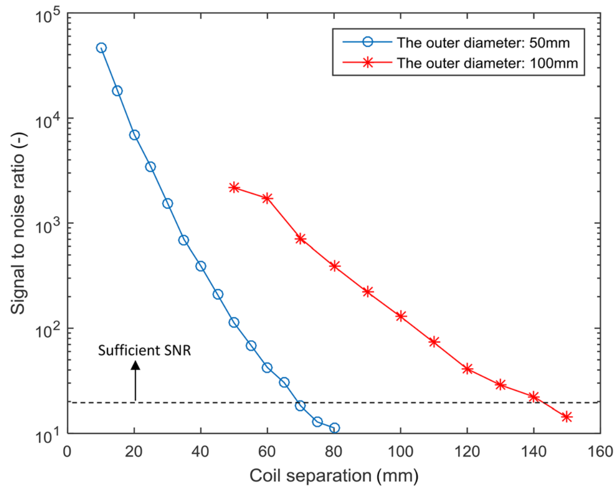

Fig. 5 Effect of the coil separation on SNR

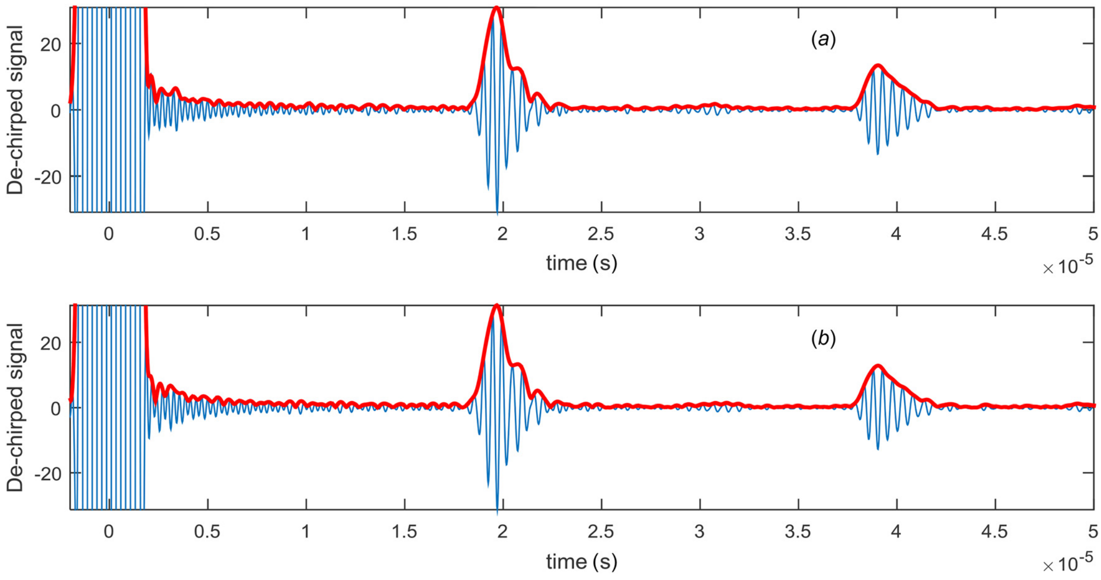

Fig. 6 The comparison of the dechirped signals with/without the insulator: (*a*) without the insulator and (*b*) with the insulator of 50 mm thickness

thickness measurement performance of the ICTS, the ultrasonic measurements are also compared with a micrometer thickness measurement (shown in Fig. 4). The speed of sound in the specimen was previously evaluated by using the micrometer measurement thickness and a conventional 5 MHz ultrasonic sensor as an accurate reference. The ultrasonically measured thickness shown in Fig. 4 was calculated by using the time interval of the signal envelope peaks. The results show good performance of the thickness measurement of the ICTS. The error of the ICTS was less than 0.2 mm in these experiments, which corresponds to general measurement accuracy in nuclear power plant inspection. In all described experiments, we used flat plates as the specimen. Piping systems of nuclear power plants have complex geometries such as bends, T-junctions, and small diameter piping systems. The curvature of these geometries might cause a reduction of the signal strength, an investigation into this will form part of the future work.

Effect of Coil Separation. Since the ICTS is based on electromagnetic induction between coils, the SNR depends on the distance between the transmitter/receiver coil and the transducer coil. In order to quantitatively evaluate the relationship between the coil separation and the SNR, we performed experiments where the coil separation was varied as the parameter. Here, the SNR is defined as the ratio between the first echo peak and the random noise level. The specimen used in these experiments is a carbon steel plate with a thickness of 20 mm.

The experimental results are shown in Fig. 5. The SNR exponentially decreases with coil separation. The results show the same trend as in the previous study [18]. The mutual inductance between two parallel circular single-turn coils can be calculated by the Maxwell's equation [17]. This equation includes the term of $\exp(-d)$, where d represents the relative vertical distance between the centers of the coils. This is the reason why the SNR reduces exponentially. From these results, we found that the

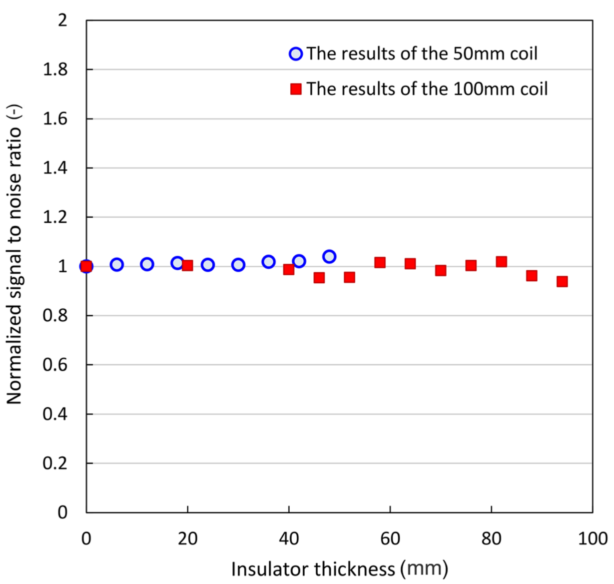

Fig. 7 SNRs with the different insulator thicknesses

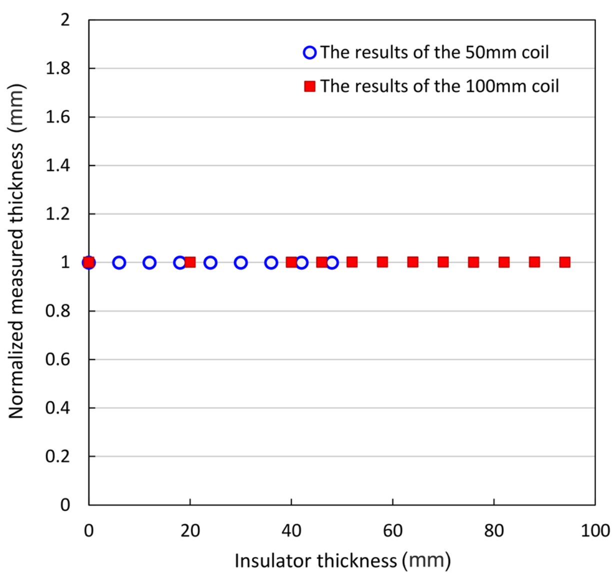

Fig. 8 The measured thickness with the different insulator thicknesses

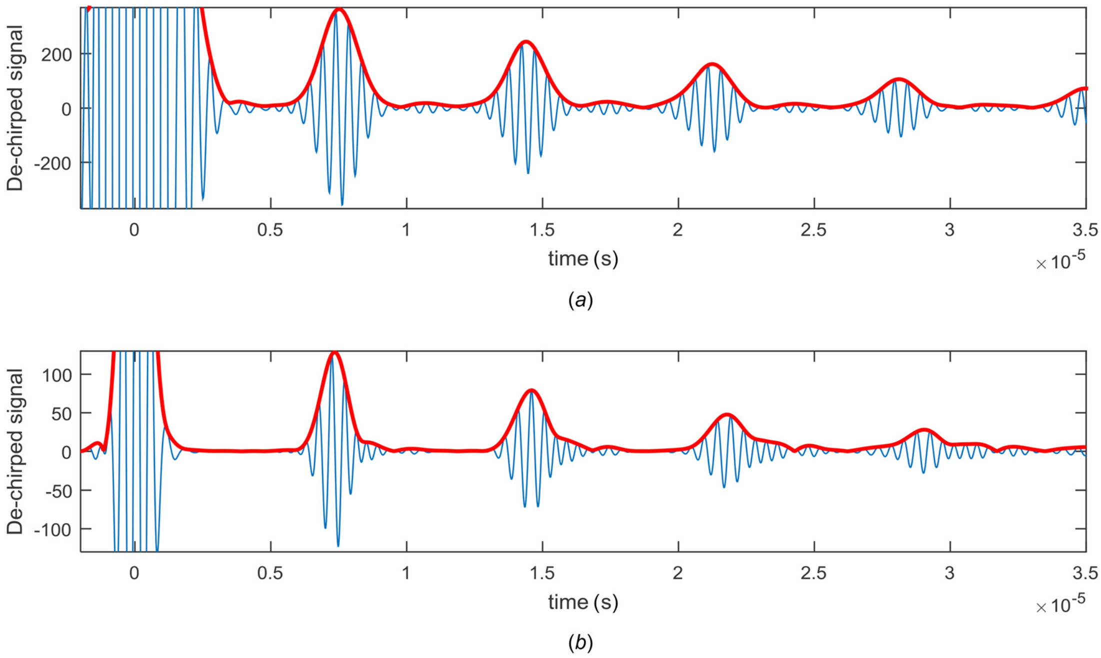

Fig. 9 The comparison of the dechirped signals in the thickness measurement of the stainless steel plate: (*a*) conventional ultrasonic sensor and (*b*) ICTS (coil separation: 35 mm)

sufficient SNR of 20, which gives an accurate thickness without an influence of cross-talk, can be obtained if the coil separation is less than 70 mm. A larger coil separation allows more flexible operation of the ICTS. As described above, the outer diameter of the coils is most effective parameter for the maximum coil separation and we, therefore, tested coils with an outer diameter of approximately 100 mm. The results of the larger coils are also shown in Fig. 5. The SNR is improved by using the larger coils and we found that the maximum noncontact measurement distance is extended to more than 140 mm. The maximum coil separation could be extended by further optimization.

Effect of Insulator. To evaluate the effect of the insulator on the SNR, we performed the measurements with and without an insulator. Silicate calcium is mainly used as the insulator material in nuclear power plants and so was used in this study. The silicate calcium insulator was placed between the transducer coil and the inspection wand as shown in Fig. 2. The thickness of the specimen used in these experiments is 60 mm. The speed of sound of the specimen was measured in advance. In all cases, the coil separation was fixed at 65 mm for the 50 mm diameter coil sensor and 100 mm for 100 mm diameter coil sensor. The dechirped signals obtained by the experiments with and without the insulator are compared in Fig. 6. There is excellent agreement between the results even though the insulator is relatively thick (50 mm).

In order to quantitatively evaluate the effect of insulator thickness on the SNR, we conducted the experiments with insulators of various thicknesses. The SNR is defined as the ratio between the first echo peak and the random noise level. Figure 7 shows the SNRs which were normalized by the SNR without the insulator. We found that the SNR becomes constant regardless of the thicknesses of the silicate calcium insulator with any changes related to the random noise levels in the measurement. The measured thicknesses obtained by using the time interval of the signal envelope peaks are shown in Fig. 8. The measured thicknesses were normalized by the micrometer measurement thickness. The ultrasonically measured thicknesses show good agreement with the micrometer measurement thickness. We also found that the there is no effect of the insulator on the thickness measurements. From these results, we confirm that it is possible to use the system for inspection without removing the insulator.

Effect of Different Inspection Material. In addition to carbon steel, stainless steel is also used as piping material in nuclear

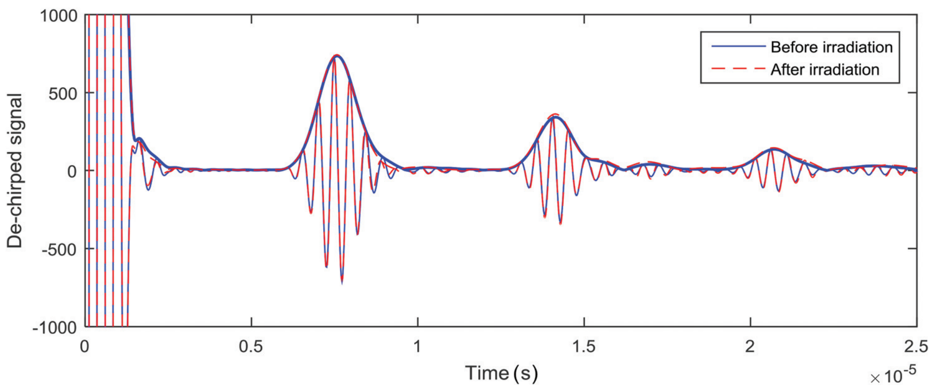

Fig. 10 The comparison of the dechirped signals with/without the irradiation

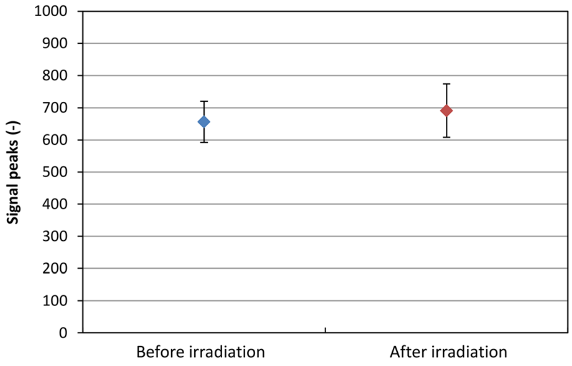

Fig. 11 The comparison of the signal peaks with/without the irradiation

power plants. We investigate the effect of using a stainless steel plate with a thickness of 20 mm. The coil separation is fixed at 35 mm for the sufficient SNR. The insulator is not used in this experiment.

The comparison of the dechirped signals by the ICTS and the conventional ultrasonic sensor is shown in Fig. 9. Good agreement between them has been confirmed from this comparison. The amplitude of the signal peaks in this experiment is around the same as the carbon steel measurement shown in Fig. 3. From these results, we confirm that the effect of this different inspection material on the SNR is negligible.

Radiation Tolerance. With an ICTS sensor permanently bonded to the surface of a pipe for a long time period, it is exposed to radiation during the plant operation. Therefore, it is essential we confirm the radiation tolerance of the ICTS here. In order to avoid the individual difference of the sensors, the same set of sensors was tested in this experiment. First, the experiment using the ICTS before irradiation is carried out. Next, the transducer coil and the piezoelectric transducer are irradiated using a radiation source. The experiment is then repeated using the

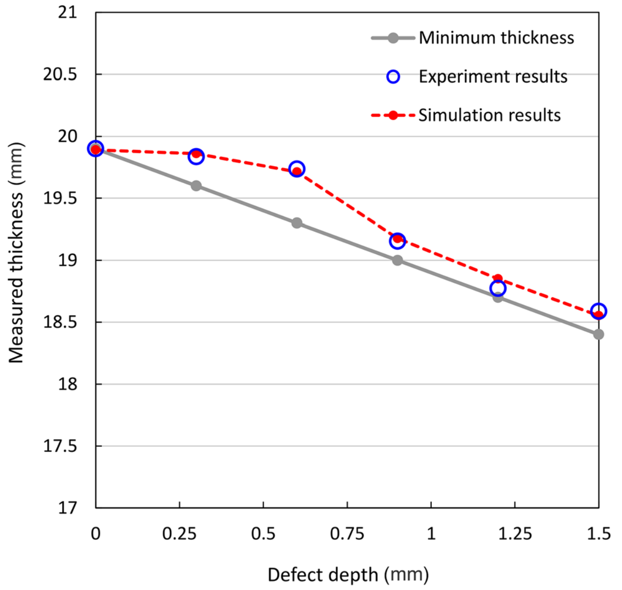

Fig. 13 The results of the wastage defect inspection by the ICTS

irradiated transducer coil and the irradiated piezoelectric transducer under the same experimental conditions. The specimen in this experiment is a 20 mm thick carbon steel plate. For the irradiation of the transducer coil and the piezoelectric transducer, gamma rays from Co-60 were used as the radiation source. The total exposure is 18 kGy which corresponds to the total exposure dose of the main steel pipe for 10 years in the primary containment vessel.

The dechirped signals before and after the irradiation are compared in Fig. 10. Excellent agreement between both signals has been obtained. The first echo signal peaks obtained from ten repeat measurements are compared in Fig. 11. The mean values agreed with each other within the standard deviations. From these

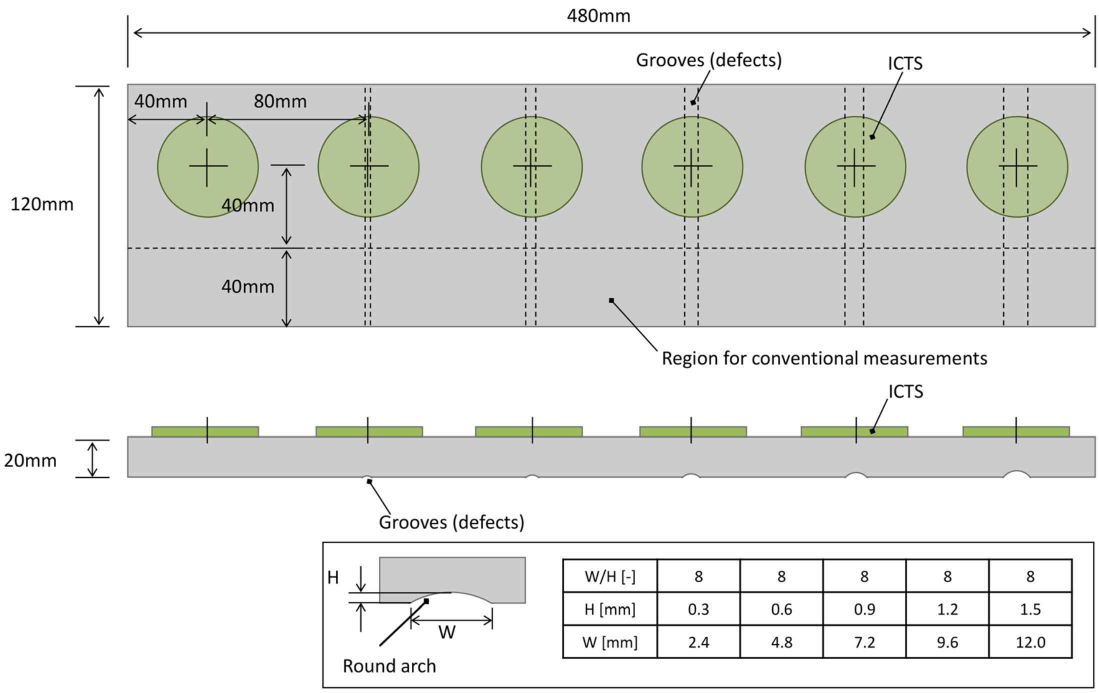

Fig. 12 A schematic view of the wastage defect test

results, we found that the ICTS has sufficient radiation durability for nuclear power plant inspections.

Measurement Accuracy for Wastage Defect. In these experiments, we investigate the measurement accuracy of the ICTS for LDI wastage defects. The specimen is a 20 mm thick carbon steel plate. As shown in Fig. 12, there are five different grooves on the underside of the plate which represent the LDI wastage defects. These grooves have the same aspect ratio between the width and depth. The depth of these grooves is 0.3, 0.6, 0.9, 1.2, and 1.5 mm. The speed of sound of the specimen was previously measured by the micrometer and the commercial ultrasonic transducer. In the inspection of the pipe-wall thinning, it is most important to measure the minimum thickness. To do this, we evaluate the thickness by using the beginning of the first echo and the speed of sound, instead of the time interval between the signal envelope peaks. In all cases, the coil separation is fixed at 20 mm, where the SNR becomes sufficiently high. In order to confirm the confidence of the measurement results, an ultrasonic simulation is also conducted at the same time. The ultrasonic simulation code is based on the finite-difference time-domain (FDTD) method [20–22]. For

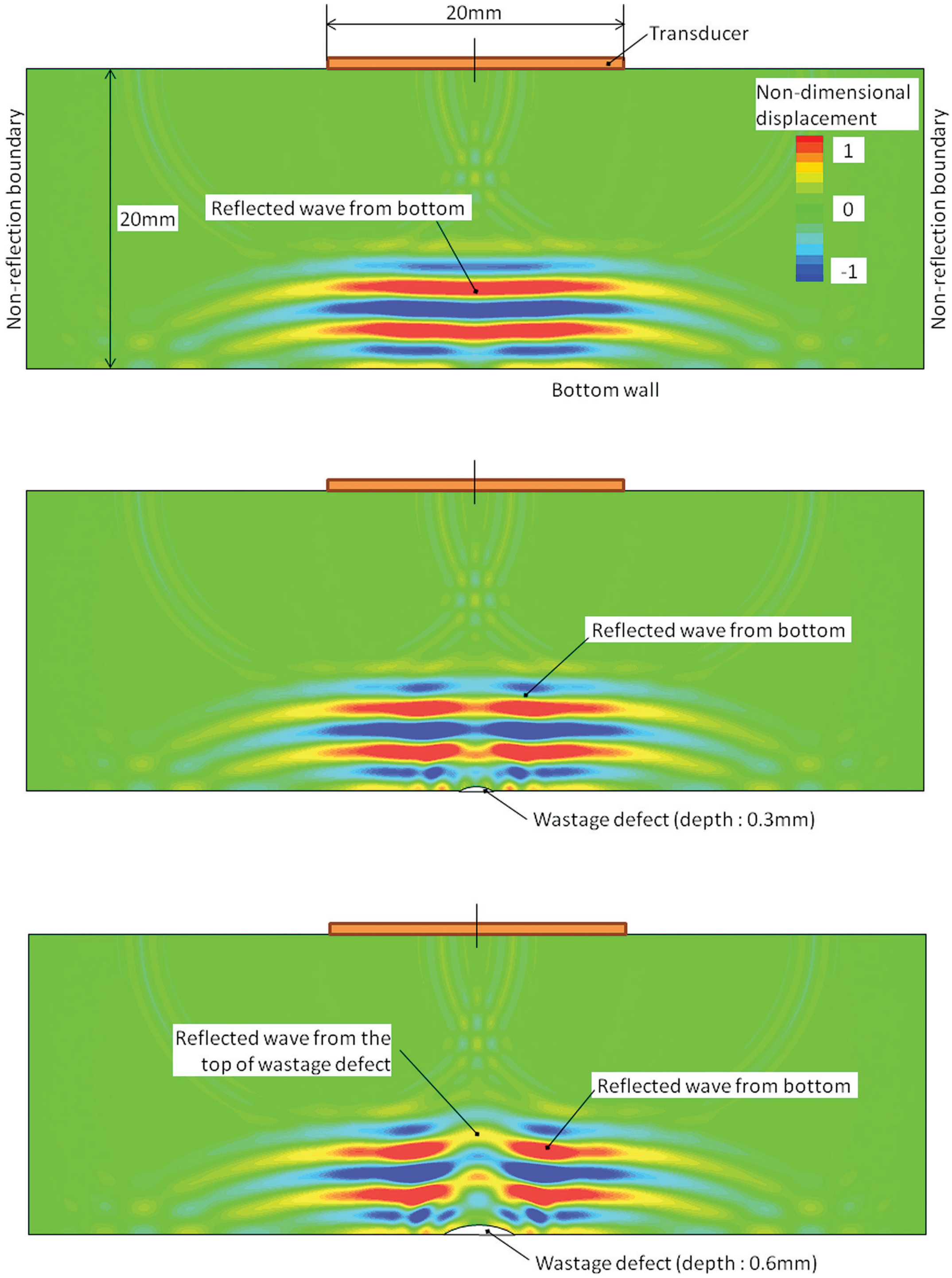

Fig. 14 The displacement distribution of the simulation result at 5×10^{-6} s

sufficiently accurate simulations, the mesh size is set to 0.1 mm, which corresponds to approximately 30 meshes per wavelength. For stable calculations, the Courant number of these simulations is set to 0.84.

The ultrasonically measured thickness is compared to the simulation result in Fig. 13. The measured thickness obtained from the defects whose depth is more than 0.9 mm showed quantitative agreement with the minimum thickness. The difference between the minimum thickness and the measured thickness was less than 0.2 mm. In the measurements of the 0.3 and 0.6 mm defects, however, the measured thickness shows a different trend. The simulation results, shown in Fig. 14, can be used to explain the reason for this. The color represents the displacement at the vertical direction. These displacement distributions show the ultrasonic waves which are reflected from the bottom and the defect. In the results of the 0.3 and 0.6 mm defects, the reflected wave from the defect is obviously small compared to the reflected wave from the bottom. On the other hand, in the results of 0.9, 1.2, 1.5 mm defect, the reflected wave from the defect is comparable to the reflected wave from the bottom. This is the reason why the measured thickness of the 0.3 and 0.6 mm defects shows different trend from the others.

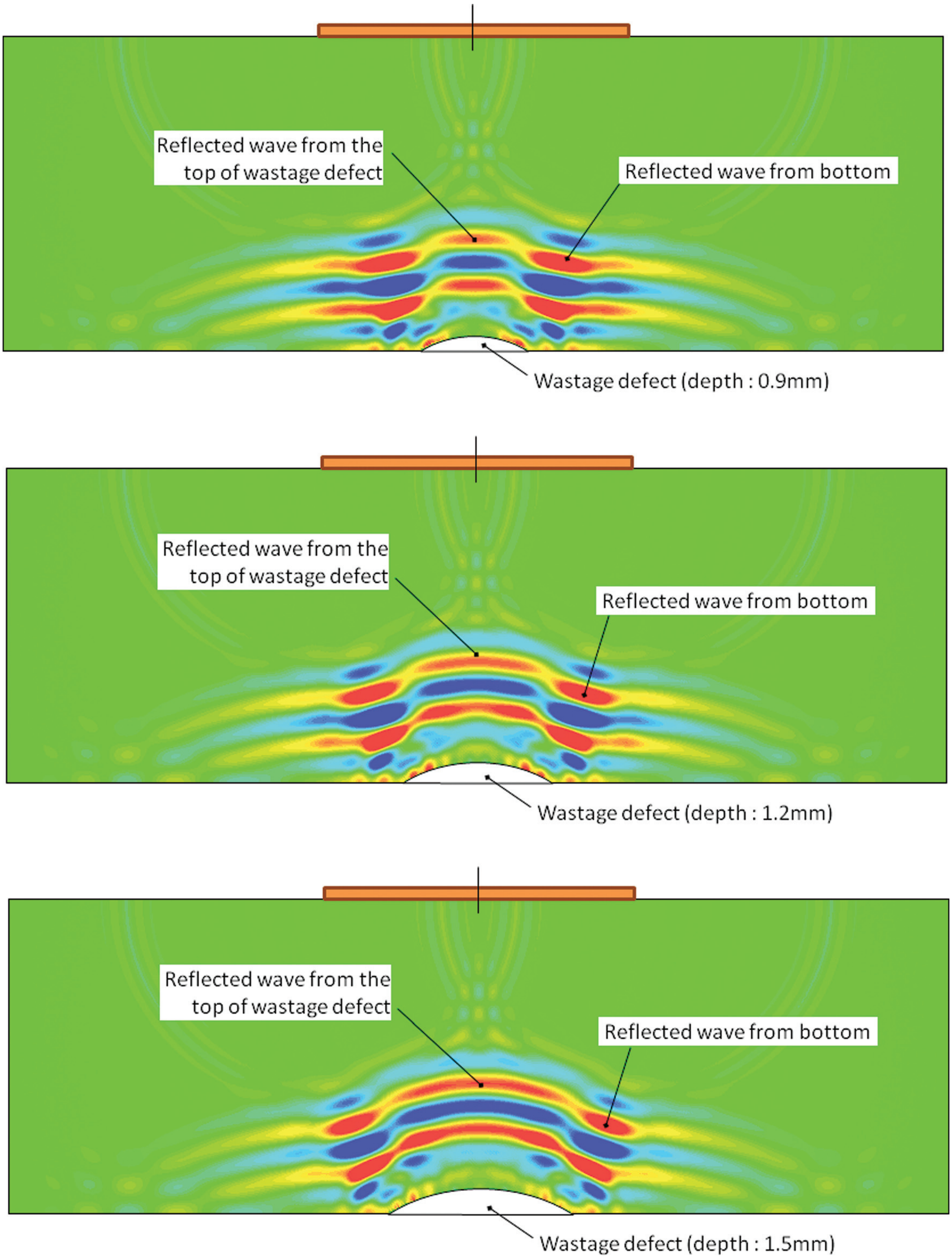

Fig. 14 Continued

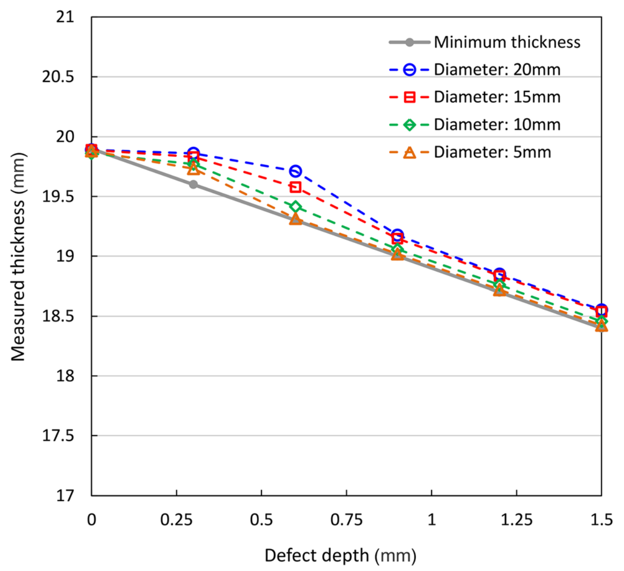

Fig. 15 Simulation results showing the effect of the transducer diameter on wastage defect inspection

The simulation results imply that smaller transducer would be better for the measurements of 0.3 and 0.6 mm defects. To confirm this, we therefore performed the simulations with the smaller transducers. The measured thickness obtained by the simulations is shown in Fig. 15. From these results, we found that all of the defects in these experiments could be measured within 0.2 mm difference from the minimum thicknesses if the transducer diameter is less than 10 mm.

Conclusions

In this study, we investigated the applicability of an ICTS developed at the University of Bristol to nuclear power plant inspection, particularly inspection of pipe-wall thinning. We can conclude that:

(1) The ICTS is applicable to wall-thickness measurement across a range of wall-thinning inspection thickness.
(2) The maximum coil separation is 70 mm with a 50 mm diameter coil design and larger coils enable a larger separation (up to 140 mm with a 100 mm diameter coil).
(3) Silicate calcium insulator material, commonly used in nuclear power plants, does not affect the measurement by the ICTS regardless of its thickness. This means that a thickness measurement can be performed with the system without removing the insulator from the pipe.
(4) The difference between the SNRs for carbon steel and stainless steel measurements is negligible.
(5) Irradiation of the transducer coil and the piezoelectric transducer did not affect the performance of the system and we confirmed sufficient radiation durability of the ICTS.
(6) The ICTS shows good performance regarding the wastage defect measurement in the experiments using the simulated LDI defects. For the inspection of small defects (less than 0.6 mm deep), a smaller diameter transducer is required. If the small diameter transducer is applied to the inspection with the sufficient SNR, the thinnest thickness can be measured within 0.2 mm difference.

These experimental results showed that the ICTS has possibility to enable the wall-thinning inspection without removing the insulator. It should be noted that to apply the ICTS to the high temperature piping system of the nuclear power plant, further development regarding high temperature durability will be necessary. Also the piping system of nuclear power plants has complex geometries such as bend, T-junction and small diameter piping systems. Future work will confirm the applicability of the ICTS to such complex geometries.

Nomenclature

B = chirp bandwidth, s
d = relative vertical distance between the centers of the coils, m
f_c = central frequency, Hz
S = chirp signal
t = time, s
T = duration of chirp signal, s
w = window function having a unit amplitude and duration of T

References

[1] Cegla, F. B., Cawley, P., Allin, J., and Davies, J., 2011, "High-Temperature (>500° C) Wall Thickness Monitoring Using Dry-Coupled Ultrasonic Waveguide Transducers," IEEE Trans. Ultrason., Ferroelectr. Freq. Control, **58**(1), pp. 156–167.
[2] Honarvara, F., Salehia, F., Safavib, V., Mokhtaria, A., and Sinclair, A. N., 2013, "Ultrasonic Monitoring of Erosion/Corrosion Thinning Rates in Industrial Piping Systems," Ultrasonics, **53**(7), pp. 1251–1258.
[3] United States Nuclear Regulatory Commission, 1986, "Feedwater Line Break," Information Notice No. 86-106.
[4] United States Nuclear Regulatory Commission, 2006, "Secondary Piping Rupture at the Mihama Power Station in Japan," Information Notice No. 2006-08.
[5] Chexal, B., Horowitz, J., and Dooley, B., 1998, "Flow-Accelerated Corrosion in Power Plants," EPRI, Palo Alto, CA, Report No. EPRI-TR-106611-R1.
[6] Horowitz, J., 2006, "Determining Piping Wear Caused by Flow-Accelerated Corrosion From Single-Outage Inspection Data," EPRI, Palo Alto, CA, Report No. 1013012.
[7] Zander, A., and Nopper, H., 2008, "The COMSY: Code for the Detecting of Piping Degradation Due to Flow-Accelerated Corrosion," ASME Paper No. PVP2008-61823.
[8] Sanchez-Caldera, L. E., Griffith, P., and Rabinowicz, E., 1988, "The Mechanism of Corrosion–Erosion in Steam Extraction Lines of Power Stations," ASME J. Eng. Gas Turbines Power, **110**(2), pp. 180–184.
[9] Munson, D., and Horowitz, J., 2007, "Recommendations for an Effective Flow-Accelerated Corrosion Program," EPRI, Palo Alto, CA, Report No. 1015425.
[10] Smith, D., and Horowitz, J., 2014, "The Role of CHECWORKS in an Effective FAC Program," ASME Paper No. ICONE22-30854.
[11] Jang, S., Jo, H., Cho, S., Mechitov, K., Rice, J. A., Sim, S. H., Jung, H. J., Yun, C. B., Spencer, J., Billie, F., and Agha, G., 2010, "Structural Health Monitoring of a Cable-Stayed Bridge Using Smart Sensor Technology: Deployment and Evaluation," Smart Struct. Syst., **6**(5–6), pp. 439–459.
[12] Want, R., 2006, "An Introduction to RFID Technology," IEEE Pervasive Comput., **5**(1), pp. 25–33.
[13] Lenaerts, B., and Puers, R., 2005, "Inductive Powering of a Freely Moving System," Sens. Actuators, A, **123–124**, pp. 522–530.
[14] Lenaerts, B., and Puers, R., 2007, "An Inductive Power Link for a Wireless Endoscope," Biosens. Bioelectron., **22**(7), pp. 1390–1395.
[15] Greve, D. W., Hoon, S., Yue, C. P., and Oppenheim, I. J., 2007, "An Inductively-Coupled Lamb Wave Transducer," IEEE Sens. J., **7**(2), pp. 295–301.
[16] Greve, D. W., Oppenheim, I. J., and Zheng, P., 2007, "Inductive Coupling for Wireless Lamb Wave and Longitudinal Wave Transducers," 6th International Workshop on Structural Health Monitoring, Stanford, CA, Sept. 11-13, pp. 1038–1045.
[17] Zhong, C. H., Croxford, A. J., and Wilcox, P. D., 2013, "Investigation of Inductively-Coupled Ultrasonic Transducer System for NDE," IEEE Trans. Ultrason., Ferroelectr. Freq. Control, **60**(6), pp. 1115–1125.
[18] Zhong, C. H., Croxford, A. J., and Wilcox, P. D., 2014, "Remote Inspection System for Impact Damage in Large Composite Structure," Proc. R. Soc. London, Ser. A, **470**(2173), p. 20140631.
[19] Michaels, J. E., Lee, S. J., Croxford, A. J., and Wilcox, P. D., 2013, "Chirp Excitation of Ultrasonic Guided Waves," Ultrasonics, **53**(1), pp. 265–270.
[20] Alterman, Z., and Karal, F. C., Jr., 1968, "Propagation of Elastic Waves in Layered Media by Finite Difference Methods," Bull. Seismol. Soc. Am., **58**(1), pp. 367–398.
[21] Virieux, J., 1984, "SH-Wave Propagation in Heterogeneous Media; Velocity-Stress Finite-Difference Method," Geophysics, **49**(11), pp. 1933–1942.
[22] Chew, W. C., and Liu, Q. H., 1996, "Perfectly Matched Layers for Elastodynamics: A New Absorbing Boundary Condition," J. Comput. Acoust., **4**(4), pp. 341–359.